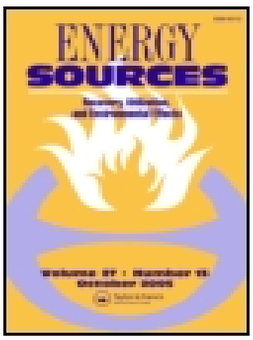

Energy Sources, Part A: Recovery, Utilization, and Environmental Effects

ISSN: 1556-7036 (Print) 1556-7230 (Online) Journal homepage: http://www.tandfonline.com/loi/ueso20

Experimental and numerical investigation of effects of CNG and gasoline fuels on engine performance and emissions in a dual sequential spark ignition engine

Ahmet Alper Yontar & Yahya Doğu

To cite this article: Ahmet Alper Yontar & Yahya Doğu (2018): Experimental and numerical investigation of effects of CNG and gasoline fuels on engine performance and emissions in a dual sequential spark ignition engine, Energy Sources, Part A: Recovery, Utilization, and Environmental Effects, DOI: 10.1080/15567036.2018.1495783

To link to this article: https://doi.org/10.1080/15567036.2018.1495783

Published online: 11 Jul 2018.

ENERGY SOURCES, PART A: RECOVERY, UTILIZATION, AND ENVIRONMENTAL EFFECTS
https://doi.org/10.1080/15567036.2018.1495783

Taylor & Francis
Taylor & Francis Group

Experimental and numerical investigation of effects of CNG and gasoline fuels on engine performance and emissions in a dual sequential spark ignition engine

Ahmet Alper Yontar [a] and Yahya Doğu [b]

[a]Department of Automotive Engineering, Mersin University, Mersin, Turkey; [b]Department of Mechanical Engineering, Kırıkkale University, Kırıkkale, Turkey

ABSTRACT

Compared to widening usage of CNG in commercial gasoline engines, insufficient but increasing number of studies have appeared in open literature during last decades while engine characteristics need to be quantified in exact numbers for each specific fuel converted engine. In this study, a dual sequential spark ignition engine (Honda L13A4 i-DSI) is tested separately either with gasoline or CNG at wide open throttle. This specific engine has unique features of dual sequential ignition with variable timing, asymmetrical combustion chamber, and diagonally positioned dual spark-plug. Thus, the engine led some important engine technologies of VTEC and VVT. Tests are performed by varying the engine speed from 1500 rpm to 4000 rpm with an increment of 500 rpm. The engine's maximum torque speed of 2800 rpm is also tested. For gasoline and CNG fuels, engine performance (brake torque, brake power, brake specific fuel consumption, brake mean effective pressure), emissions (O_2, CO_2, CO, HC, NO_x, and lambda), and the exhaust gas temperature are evaluated. In addition, numerical engine analyses are performed by constructing a 1-D model for the entire test rig and the engine by using Ricardo-Wave software. In the 1-D engine model, same test parameters are analyzed, and same test outputs are calculated. Thus, the test and the 1-D engine model are employed to quantify the effects of gasoline and CNG fuels on the engine performance and emissions for a unique engine. In general, all test and model results show similar and close trends. Results for the tested commercial engine show that CNG operation decreases the brake torque (12.7%), the brake power (12.4%), the brake mean effective pressure (12.8%), the brake specific fuel consumption (16.5%), the CO_2 emission (12.1%), the CO emission (89.7%). The HC emission for CNG is much lower than gasoline. The O_2 emission for CNG is approximately 55.4% higher than gasoline. The NO_x emission for CNG at high speeds is higher than gasoline. The variation percentages are the averages of the considered speed range from 1500 rpm to 4000 rpm.

KEYWORDS

1-D engine modeling; CNG; Dual sequential spark ignition engine; emission; engine performance; engine test; gasoline; wide open throttle

Introduction

During the last decades, engine technology has been experiencing many superior cutting-edge developments like HCCI, RCCI, PCCI, SACI, VTEC, VVT while usage of alternative fuels on new technology engines rapidly widens. The emission regulations and fuel economy put ever-increasing pressure on automotive industry not only to develop new engine technologies but also to search alternative fuel usage in the current new technology engines. Among many alternative fuels for gasoline engines, CNG, LNG, and LPG are the widely available and used ones. Due to its high H/C ratio, high research octane number, combustion advantages, and competitive cost as well; CNG is

CONTACT Ahmet Alper Yontar alperyontar17@gmail.com

Color versions of one or more of the figures in the article can be found online at www.tandfonline.com/ueso.

the most popular alternative fuel varieties for conventional liquid automobile fuels. The number of CNG vehicles in the world has reached about 23 million (http://www.iangv.org/current-ngv-stats/ ,2017.06.20). CNG usage in engines has many benefits like lower knock tendency, higher compression ratio, uniform mixture formation, longer lubrication oil life, mitigated greenhouse gas emissions, reduced cold start problem, and improved fuel economy (Cho and Bang-Quan 2007).

As a consequence of all kinds of advantages of CNG, increasing number of works about natural gas conversions on gasoline and diesel engines have been performed during last decades. When CNG as an alternative fuel will be used in an engine, which is originally designed for gasoline, it becomes a need to know and determine engine performance and emissions for CNG usage. Engine characteristics for CNG differ depending on engine's specific design. In order to determine benefits of CNG usage, engine characteristics need to be quantified in exact numbers for each specific engine while some general trends for conventional engines are known for CNG usage (Cho and Bang-Quan 2007). Compared to widening usage of CNG in gasoline engines, limited but ever-increasing number of studies have been appearing in open literature in recent years. Some of them are evaluated below in terms of testing and modeling.

One of the CNG tests was done by Varde and Asar (2001). They experimentally studied burning characteristics of homogeneous natural gas charge in a spark ignition engine. They reported that the burning speed for natural gas was slower than gasoline mixtures. They investigated flame kernel propagation depending on mixture stoichiometry, engine load, and speed.

Aslam et al. (2006) tested a retrofitted spark ignition engine fueled with gasoline and CNG at different loads (25–100%) and speeds (1500-5500 rpm). They concluded that, in general, CNG usage gave lower specific fuel consumption, higher fuel conversion efficiency, lower CO and HC emissions, and higher NO_x emission.

Geok et al. (2009) tested a sequential port injection natural gas engine at wide open throttle. The volumetric efficiency decreased 4–10% for CNG operation. CNG sequential port injection system improved brake specific fuel consumption.

Zheng et al. (2009) experimentally showed that compression ratio has a significant influence on the engine performance, combustion, and emission for a CNG direct injection engine. They reported that the duration of flame development rapid combustion and total combustion decrease on increasing the compression ratio. The optimum value of compression ratio of twelve is suggested for CNG.

Pipitone and Beccari (2009) tested a single fuel of gasoline and CNG and a double-fuel injection of both fuels to investigate their benefits. After performing many tests, they reported that, compared to pure gasoline and CNG injections, when both fuels are injected at stoichiometric ratio, fuel economy is considerably increased without remarkable power losses while knock resistance is strengthened.

Delpech et al. (2010) investigated effects of CNG, gasoline and concomitant injection in a turbocharged spark ignition engine. They modified compression ratio of the spark ignition engine from 9.5 to 11.5. Their tests demonstrated that engine torque for the concomitant injection mode is higher than CNG and gasoline modes because of higher volumetric and thermal efficiencies.

Jahirul et al. (2010) tested another retrofitted spark ignition engine with gasoline and CNG at loads of 50% and 80% and speeds of 1500-5500 rpm. In general, CNG usage reduced brake power, brake specific fuel consumption, emissions of HC, CO, O_2, and CO_2, while it increased brake thermal efficiency, exhaust gas temperature, and NO_x emission.

Ha, Park, and Kang (2010) tested a direct-injection engine fueled with CNG. They observed that combustion characteristics greatly improved with early injection timing for wide open throttle and with late injection timing for partial throttle openings.

Obiols et al. (2011) tested a direct injection of gasoline and a port injection of CNG in a turbocharged spark ignition engine. They reported that the engine torque for concomitant injection is higher than CNG and gasoline injections.

Movahed, Basirat, and Mirsalim (2014) developed a test rig to test an engine with a single fuel of gasoline and CNG and a mixture of them in order to search the knock prevention by supplying the

mixture. They demonstrated that the concomitant injection improves thermal efficiency. When CNG addition rate increased in the mixture, the engine power increases up to certain CNG rate, then, stays constant. The emissions consistently decreased with increasing CNG rate.

Putrasari et al. (2015) investigated the effect of CNG usage on engine performance and emissions at partial load conditions for a single-spark ignition engine. They tested a specific engine with gasoline and CNG in the speed range of 2000–4500 rpm and throttle range of 25–80%. For the tested conditions, CNG gave lower emissions while gasoline provides higher engine performance.

Meanwhile, some testing studies have appeared about hydrogen enriched CNG (HCNG). Wang et al. (2012) also experimentally worked on HCNG fuel for SI engine and investigated effects of ignition timing, hydrogen fraction, engine speed, throttle opening, coolant, and oil temperature on lean combustion limit.

Lim et al. (2013) tested a heavy-duty SI engine fueled with HCNG. They reported the increased thermal efficiency decreased NO_x emission with increased compression ratio.

Verma et al. (2016) tested HCNG fuel in a spark ignition engine. H/C ratio is controlled with hydrogen enrichment. With increasing H/C ratio in natural gas, thermal efficiency rises. They demonstrated that thermal efficiency rises with increasing H/C ratio in natural gas. Furthermore, NO_x emission at 55 Nm torque becomes highest for H/C ratio of 4.22, however, NO_x emission at full load has the highest value for H/C ratio of 4.5. They concluded that the mixed fuel with H/C ratio of 4.5 showed best overall engine performance.

Thipse et al. (2009) worked on CFD simulation of a six-cylinder HCNG engine to identify the optimum hydrogen-CNG blend.

In terms of modeling studies of CNG engines, D'Errico and Lucchini (2005) developed a multi-zone thermo-fluid dynamic combustion model for CNG. With a detailed chemical kinetic approach, the laminar flame velocity correlation was improved and the turbulent, premixed combustion mechanism was examined in detail.

Bozza et al. (2008) simulated the scavenging and combustion process in a gasoline and natural gas fueled two-stroke engine with a modified version of the KIVA3V code. They compared results with experimental data, quantified the fresh mixture short-circuiting, and analyzed the development of the natural gas combustion process for a diluted mixture.

Yadollahi and Boroomand (2013) modeled in-cylinder combustion in AVL FIRE software to investigate effects of combustion chamber geometry and injector shape in a spark ignition engine for CNG usage. They analyzed five piston head shapes and two injector types. They determined the most suitable piston head shape and injector type for CNG usage.

Xu et al. (2014) used GT-Power to study 1-D simulation of a Cummins ISX heavy duty, dual-fuel, natural gas-diesel engine. They validated the simulation through experimental results and determined the ignition delay and injection timing through an iterative calculation based on Start of Combustion (SOC) and a predictive ignition delay correlation.

Baratta et al. (2018) employed 1-D and 3-D simulations and tests for a CNG fueled diesel engine. They said EGR could increase the CNG engine efficiency.

As the engine modeling software developed, the agreements between test results and the modeling software results have been experienced in many studies in literature in terms of the 1-D engine modeling (Alqahtani, Shokrollahihassanbarough, and Wyszynski 2015; Boretti and Jiang 2014; Hooper, Al-Shemmeri, and Goodwin 2012; Mahrous et al. 2009; Sjöberg and Dec 2004; Yontar and Doğu 2016) and the in-cylinder combustion modeling (Basha and Gopal 2009).

Sjöberg and Dec (2004) investigated effects of intake temperature and combustion phasing for premixed and DI HCCI Engine via experiment and cycle simulation in Ricardo-Wave. Their results showed that the amount of charge heating/cooling that occurs due to heat-transfer during the induction period can be computed from changes in the volumetric efficiency.

Mahrous et al. (2009) also employed Ricardo-Wave software to analyze the influence of the variable valve timing strategy on the gas exchange process and engine parameters of a 4-valve HCCI engine for gasoline.

Hooper, Al-Shemmeri, and Goodwin (2012) successfully applied Ricardo-Wave software to build a 1-D engine model for multi-fuel (indolene, kerosene JET A-1) operation.

Boretti and Jiang (2014) used both Ricardo-Wave and AVL-Boost software to develop a model for a two-stroke direct injection jet ignition CNG engine. They designed coupled injection systems. Their results of engine simulations for Ricardo-Wave showed the ability to run the engine throttle less by changing the load through the quantity of fuel injected, achieving improved top fuel conversion efficiencies.

Alqahtani, Shokrollahihassanbarough, and Wyszynski (2015) compared two engine simulation software, Ricardo-Wave, and AVL-Boost for HCCI and SI GDI engines using gasoline. They calibrated the models in both software with respect to test data. They advised Ricardo-Wave than AVL Boost, for the 1-D model accuracy.

Yontar and Doğu (2016) used Ricardo-Wave to model an engine fueled with gasoline and LNG (Liquefied Natural Gas). Torque for LNG was observed to decrease by about 15% when compared to gasoline. The volumetric efficiency and the mean effective pressure for LNG usage decreased with respect to gasoline. In terms of specific fuel consumption and exhaust emissions, the use of LNG is better than gasoline.

In this study, the effects of CNG usage on engine characteristics are experimentally and numerically determined for a specific commercial engine (Honda L13A4 i-DSI) which has unique features of dual sequential ignition with variable timing, asymmetrical combustion chamber, and diagonally positioned dual spark-plug. The engine is originally manufactured for gasoline. The gasoline engine is instrumented with CNG equipment and tested with gasoline and CNG at wide open throttle for a speed range of 1500–4000 rpm. In addition to tests, numerical engine analyses are performed by constructing a 1-D model for the entire test rig and the engine by using Ricardo-Wave software. For gasoline and CNG fuels, engine performance (brake torque, brake power, brake specific fuel consumption, brake mean effective pressure), emissions (O_2, CO_2, CO, HC, NO_x and lambda), and the exhaust gas temperature are obtained from tests and 1-D model and they are evaluated. As reviewed above, there are valuable engine test results showing the effects of CNG usage on engine characteristics for some engines. This study presents test and model results for a dual spark ignition engine. Engine testing procedure and 1-D engine modeling process are explained as follows before evaluating the results.

Experimental setup

In the experimental work, a dual sequential spark ignition engine is tested by measuring the engine performance and emissions. The schematic of the engine test rig is shown in Figure 1. The test rig mainly consists of four components; engine, eddy-current dynamometer, emission measurement unit, and instrumentation-control unit.

The test engine is a commercially available dual sequential spark ignition engine which is Honda L13A4 i-DSI. The main specifications of the engine are summarized in Table 1. The engine is originally designed for gasoline fuel. The Honda L13A4 i-DSI engine has unique features of dual sequential ignition with variable timing, asymmetrical combustion chamber, and diagonally positioned dual spark-plug. Thus, the engine led some important engine technologies of VTEC and VVT (Migita et al. 2002; Nakayama et al. 2001). As presented in a technical review (Nakayama et al. 2001), the engine has four cylinders with an intake valve and an exhaust valve in each cylinder. Engine's intake port is designed for high swirl ratio (1.10–1.36) and tumble ratio (1.30–1.58); thus, turbulence at the compression time increases and the flame propagation is fast. Fuel is injected into the intake port behind the intake valve; thus, the fuel-air mixture is fed into the cylinders. Unlike usual engines, the engine has two spark plugs per cylinder. The dual spark plugs located diagonally on each

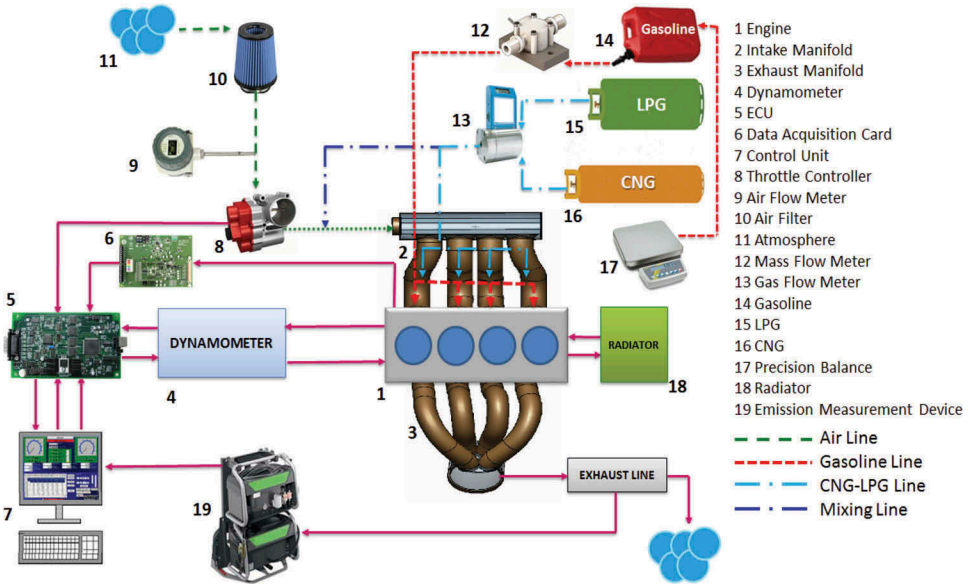

Figure 1. Photograph and schematic of engine test rig.

Table 1. Specifications of the test engine.

Engine model	Honda L13A4 i-DSI
Displacement, cc	1339
Bore, m	0.073
Stroke, m	0.080
Compression ratio	10.8:1
Number of cylinders	4
Max. torque at 2800 rpm, Nm	119
Max. power at 5700 rpm, kW	63

cylinder. One spark plug is closer to the intake valve while the other is at the exhaust valve side. This feature enhances flame formation and propagation into the entire cylinder and yields increased combustion efficiency and decreased HC emission. The dual spark plugs ignite at the same time at the idle state and above 4000 rpm. At other engine speeds, the spark plugs ignite at different times. The ignition time difference for spark plugs is determined by the electronic control unit (ECU) of the engine between 2 and 5 CAD depending on the engine speed. Another unique feature of the engine is that the combustion chamber is such asymmetrically shaped that it produces more turbulence/swirl/tumble resulting in a more homogeneous air-fuel mixture and better combustion. The engine has higher compression ratio arising from both reduced angle between the intake and the exhaust valves, complex shape of the combustion chamber and pent-roof head. The combined effect of all these design features is that the premixed flame passes the exhaust valve and propagates into combustion chamber without forming autoignition (Nakayama et al. 2001).

The engine is coupled with an eddy-current dynamometer which has measurement capability of a maximum 100 kW power and 500 Nm torque. The test rig is equipped with necessary instrumentations, sensors, actuators, and data transmitters. The data is collected on a data acquisition card. The control unit keeps the engine speed constant for a prescribed throttle opening by adjusting the dynamometer load. The engine test is carried out by measuring physical parameters (speed, brake torque, brake power, fuel consumption, intake air flow rate, temperatures) in a time interval of 0.5 seconds. Meantime, exhaust emissions (O_2, CO_2, CO, HC, NO_x, and lambda) are measured and recorded.

Table 2. Engine test parameters.

#	Parameters	Unit/Range
1	Speed	1500, 2000, 2500, 2800, 3000, 3500, 4000 rpm
2	Throttle opening	100%
3	Brake torque	Nm
4	Brake power	kW
5	BMEP	bar
6	BSFC	g/kWh
7	Lambda	
8	O_2	%vol
9	CO_2	%vol
10	CO	%vol
11	HC	ppmvol
12	NO_x	ppmvol
13	Exhaust gas temperature	K

The engine tests were carried out for seven engine speeds between 1500 and 4500 rpm at 500 intervals without excepting 2800 rpm. In order to prevent unstable and fluctuating engine operation during different engine loads, the minimum engine speed was considered as 1500 rpm. The maximum engine speed was set to the limit of 4000 rpm for safety during tests. The engine is tested at wide open throttle for all speeds.

For each engine speed, the engine was run for a certain amount of time to reach the steady state. Then, test data were collected for 2 minutes by recording in each 0.5 second. A large number test data was collected for each test setup conditions in order to provide dependable test readings by eliminating testing noises (such as instant transients, vibrations, fluctuations, actuator transients) and data reading noises of instrumentation sensors (such as time response, hysteresis, sensitivity). For each test setup conditions, the test results were obtained by averaging about 240 test data. The measured parameters are listed in Table 2.

The engine test results are presented in a comparative manner in the results and discussion section.

1-D engine model

The tested commercial engine is also simulated by using the Ricardo-Wave software package. In the engine simulation model, a 1-D model is built including the entire engine from the beginning of the intake line to the end of the exhaust line. Wave Build 3D and Wave Mesher 3D modules included in the Ricardo-Wave software infrastructure, it is possible to create 1-D models directly on solid geometry.

At the beginning of the engine modeling phase, dimensions of related engine parts are measured with a CMM device. Generally, the 1-D engine modeling in Ricardo-Wave software consists of the following steps (Ricardo-Suite Manual 2015).

First, each engine components (pistons, cylinders, valves, ports, engine blocks, intake and exhaust manifolds, fuel line, exhaust line, and throttle) are separately formed by defining their geometric parameters and physical properties. Then, engine components are connected to each other by defining the relevant relations. After that, the initial and boundary conditions are defined. The engine timing parameters are set in the code. In order to read the engine characteristics (pressure, temperature, emissions), sensors are located at certain points on the model. Thus, the entire 1-D engine model is built as plotted in Figure 2.

There are some important temperature values that need to be defined in the code as boundary conditions. These temperatures are piston temperature, cylinder head/wall temperature, intake/exhaust valve temperature depending on the engine speed. These constants used in the code have been determined by using the data in common literature (Mahle GmbH 2012; Heywood 1988).

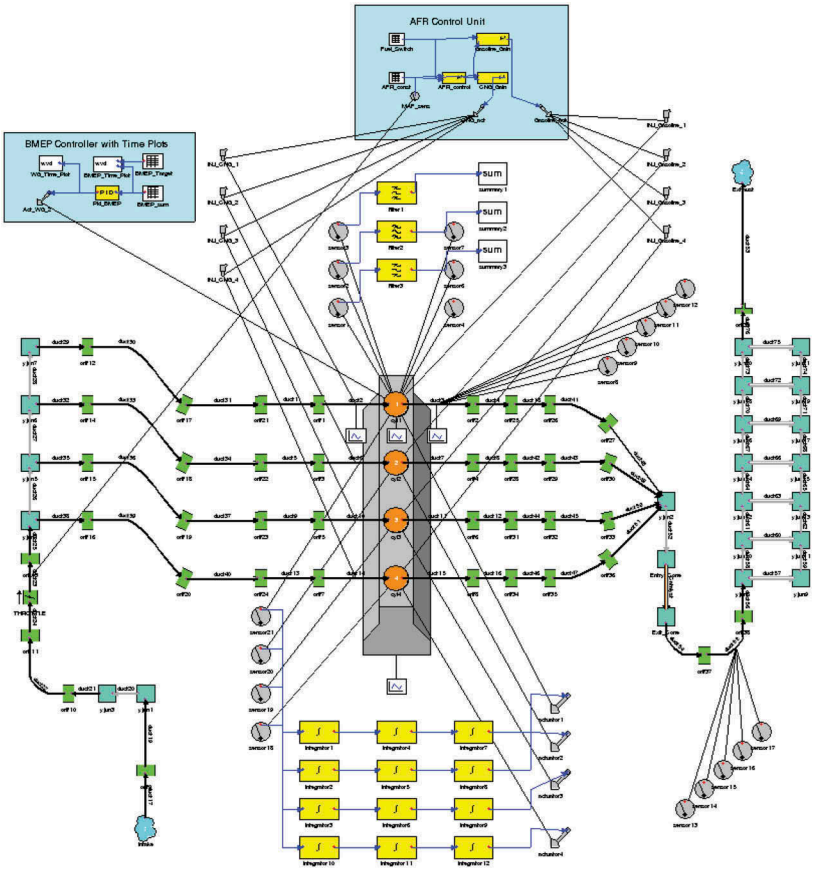

Figure 2. 1-D engine model built in Ricardo-Wave software.

In the 1-D model, Woschni heat transfer correlation (Woschni 1967) and multi-component Wiebe combustion models (Vibe 1956) are used. For emission calculations following correlations are used: Newhall correlation for CO and CO_2 (Newhall 1968), Cheng correlation for HC formation (Cheng et al. 1993), and Fenimore correlation (Fenimore 1970) and Heywood correlation (Heywood 1988) for Zeldovich formation mechanisms for NO_x.

In the Wiebe combustion model (Vibe 1956); combustion process contains three parts (pre-mixture, diffusion, and tail). The Wiebe combustion model accounts for all cycle characteristics and also considers the thermal decomposition of the combustion products. In this model, the pressure and temperature inside the cylinder vary depending on the crank angle. With the Vibe function, the calculation of the combustion curve for the entire cycle can be carried out if the average burning rate, the relative time of the maximum burning rate and the spraying rate are known. For spark ignition engines, the combustion duration in the Wiebe model ranges from 0.005 s to 0.016 s.

In the 1-D model, in order to define port injection, injection timing, and ignition timing, a Matlab code is written. This code is transferred to signal processing and control elements in Ricardo-Wave software. As shown in Figure 2, in the software, torque smart controller, AFR controller, and BMEP controller panels are built for this purpose.

The 1-D model analysis is run for engine test conditions. For each engine speed, the analysis is run for 300 engine cycles in order to ensure fully developed steady-state conditions before reading the data. The time step multiplier and the convergence criterion were set to 0.1 and 0.001, respectively.

As in the engine test procedure, same parameters of initial and boundary conditions are defined in the 1-D engine model. In the engine model, same test parameters are analyzed and same test outputs are calculated.

Results and discussion

The engine is tested with gasoline and CNG at wide open throttle for seven engine speeds between 1500 and 4500 rpm at 500 intervals without excepting 2800 rpm. The 1-D engine model is also run for the test conditions. The results obtained from the engine test and the model are presented with respect to engine speed in a comparative manner by evaluating brake torque (Figure 3), brake power (Figure 4), brake mean effective pressure (BMEP) (Figure 5), brake specific fuel consumption (BSFC) (Figure 6), lambda (Figure 7), O_2 (Figure 8), CO_2 (Figure 9), CO (10), HC (Figure 11), NO_x (Figure 12) and exhaust gas temperature (Figure 13). It should be kept in mind that the engine is originally designed for the gasoline fuel. Thus, the characteristics of a commercial engine for gasoline and CNG usage are quantified.

As seen in Figure 3, the brake torque for both gasoline and CNG has a smooth increasing and decreasing trend with a peak value at 2800 rpm. The torque curves have a smooth convex parabolic shape and show the known behavior for naturally aspirated engines (Heywood 1988). Up to peak torque value, the rising amount of air-fuel intake with increasing speed rises the torque and all kinds of frictional loses, as well. Since the torque increment at moderately low speeds is more pronounced than the frictional loses, the torque increases with speed up to a peak value. At a certain speed, due to the less amount of combustion duration in addition to enhanced frictional loses become dominant, then, the torque starts to fall.

Almost for all speeds, when the engine is run with CNG, it gives 12.7% less torque than gasoline. Since CNG in gas phase is injected into the intake manifold, the amount of intake air reduces, and, thus, the volumetric efficiency. For the gasoline, the volumetric efficiency is higher due to vaporization cooling effect. Mainly, the volumetric efficiency for CNG is less than gasoline. This yields less torque.

As plotted in Figure 3, the engine has a maximum catalog torque of 119 Nm at 2800 rpm for gasoline. The trend of torque curve gives the maximum torque at this speed. The maximum torque of 116.7 Nm and 99.2 Nm are measured at 2800 rpm for gasoline and CNG, respectively. The

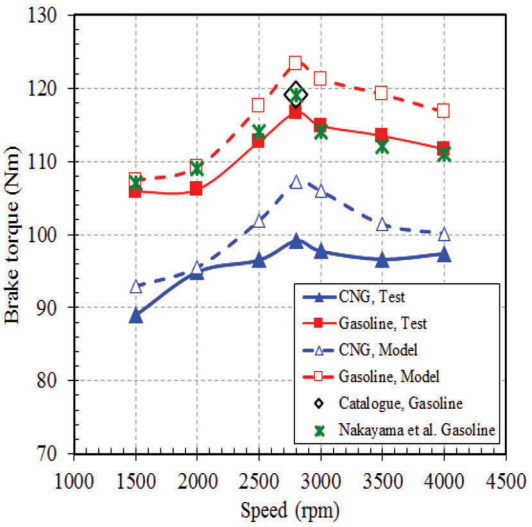

Figure 3. Brake torque.

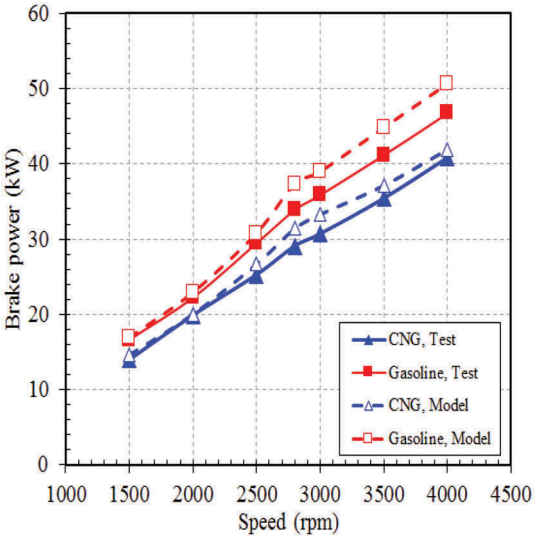

Figure 4. Brake power.

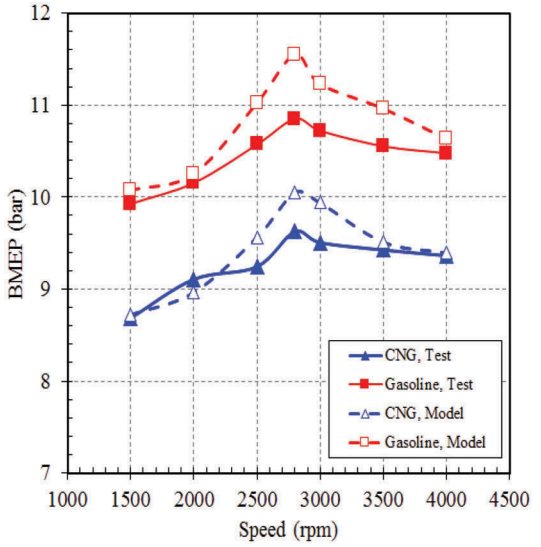

Figure 5. BMEP.

measured maximum torque for gasoline is very close to the engine catalog torque. The torque values at other speeds are also compared with available data given by Nakayama et al. (2001) as plotted in Figure 3. The close agreement validates the testing procedure.

The torque values obtained from the 1-D engine model are also plotted in Figure 3. The model results have a similar shape with the test results. Specifically, in the model, the maximum torque at 2800 rpm is calculated as 123.3 Nm and 107.2 Nm for gasoline and CNG, respectively. The torque values calculated in the 1-D engine model are 1.4–5.4% higher than the test torques depending on speed. This is an expected situation since it is difficult to include all the test conditions in the test environment into the 1-D engine model. In the test, there are many unmeasured physical losses (heat loss from engine, heat/frictional loss at manifolds, combustion efficiency). Therefore, all the real

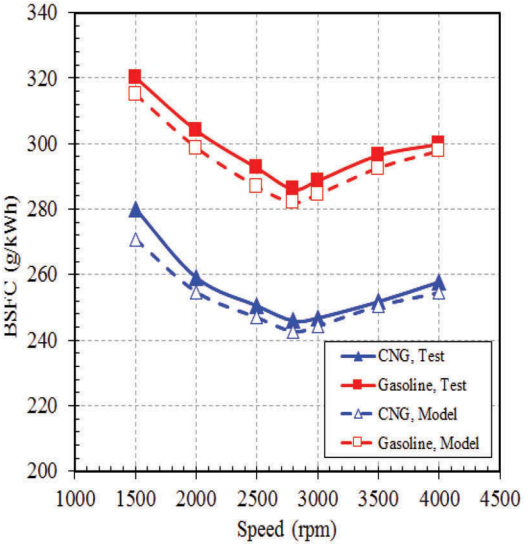

Figure 6. BSFC.

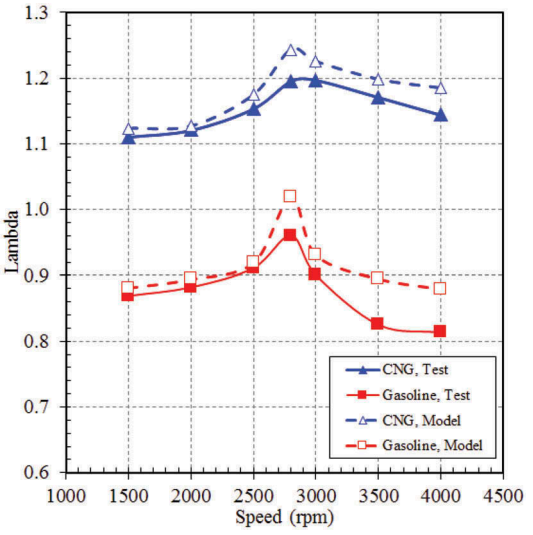

Figure 7. Lambda.

loses are not exactly included in the 1-D engine model. The torque difference between the test and the model is increasing with speed since physical losses in the test increase with speed.

In any means, the model results are very close to test results (1.4–5.4% difference). These close results verify the 1-D engine model.

Figure 4 shows that the brake power almost linearly increases with speed for both fuels due to more fuel intake into cylinders. When the speed is increased from 1500 rpm to 4000 rpm, the power increases from 16.6 kW to 46.8 kW and from 14.5 kW to 41.8 kW for gasoline test and CNG test, respectively.

As plotted in Figure 5, the BMEP (Brake Mean Effective Pressure) has similar shape and trend with the torque since the torque is calculated by using the BMEP. At the maximum torque speed of 2800 rpm, the BMEP reaches the maximum value of 10.8 bar and 9.6 bar for gasoline test and CNG

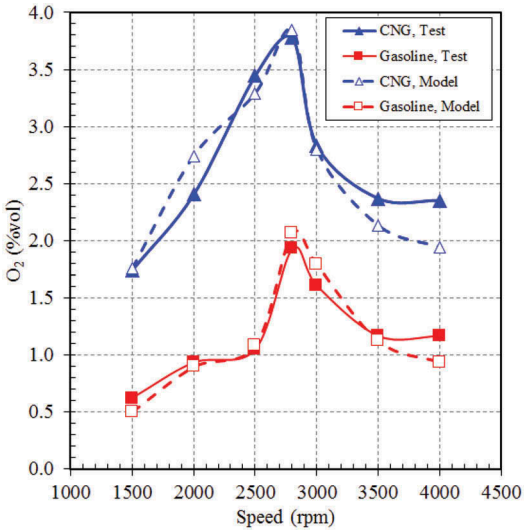

Figure 8. O_2 emission.

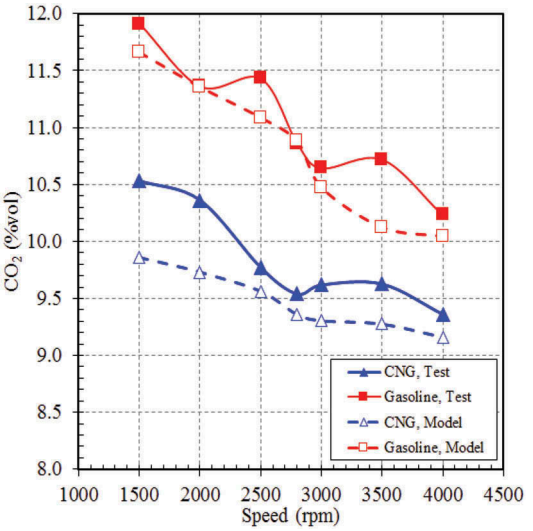

Figure 9. CO_2 emission.

test, respectively, The BMEP curves for both the test and the model closely capture the torque behavior. As explained in the torque evaluation, the volumetric efficiency for gasoline and CNG directly effects the BMEP in the similar manner.

The BSFC (Brake Specific Fuel Consumption) is also calculated and its variation with the engine speed is plotted in Figure 6. In general, it is observed that the BSFC curves have smooth concave parabolic shapes making their minimum at 2800 rpm. These behaviors of the BSFC curves are consistent with the brake torque curves. For spark ignition engines, it is known that the lowest brake specific fuel consumption is about 270 g/kWh for gasoline fuel at nominal conditions (Pulkrabek 2004). Test results show that the BSFC curves at 2800 rpm have minimum values of 286 g/kWh and 246 g/kWh for gasoline and CNG, respectively.

When all speeds are evaluated, the BSFC for CNG is approximately 16.5% less than gasoline since the power is less for CNG. The model results for the BSFC are slightly less than the test results. As

discussed above, all the physical loses during the tests have not been measured and included in the model. Thus, the fuel consumption for the same power would be less for the model.

The lambda value is plotted with respect to the engine speed for both fuels in Figure 7. The air–fuel ratio of the engine is set by the ECU. Since the engine is a commercial engine, it is not possible to intervene in the ECU. There are two ECUs on the engine for gasoline and CNG. The lambda exhibits a direction towards the lean mixing in the maximum torque range. After the maximum torque range, the behavior of the mixture is such that the fuel content is enriched as the engine speed rises for both fuels. In the usage of CNG, the engine behaves in lean mixing conditions at the operating process.

The variation of the O_2 emission is shown in Figure 8. Test curves have similar shape and trend with 1-D model curves. Around the maximum torque speed of 2800 rpm, the O_2 reaches its peak for both fuels. As the engine speed increases beyond the peak, O_2 drops rapidly. Lambda, CO_2 and CO graphs support the decrease in the O_2 emission at high engine speeds. For the considered range of engine speeds, the O_2 emission for CNG is approximately 55.4% and 55.2% higher than gasoline for the test and the model, respectively. Results obtained from tests, and analyses are very close.

Figure 9 shows that the CO_2 emission with engine speed decreases almost linearly in the range of 11.9–10.2% vol. and 10.5–9.4% vol. for gasoline and CNG, respectively. At high speeds, since the duration of engine strokes shorten, the incomplete combustion products increase. Thus, the amount of CO_2 reduces with engine speed. CNG has the highest energy/carbon ratio of any fossil fuel and, thus, produces less CO_2 per unit of energy. The C/H ratio of CNG is lower than gasoline and which in turn reduces CO_2 formation. Once again, the model and test results are reasonably close to each other. The CO_2 emission for CNG is overall 12.1% and 17.1% less than gasoline for the test and the model, respectively, when an average is taken over the speed range.

The CO emission for gasoline is very much higher than CNG, as seen in Figure 10. The emission of CO rises up with increasing engine speed. CNG has the lowest C/H ratio (C/H_{CNG}:0.25, $C/H_{gasoline}$:0.44) of any fossil fuel and produces less CO_2 and CO per unit of energy. When the

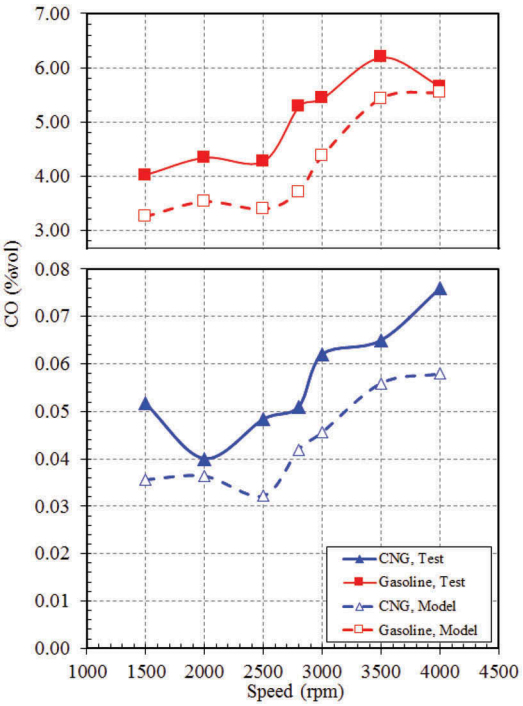

Figure 10. CO emission.

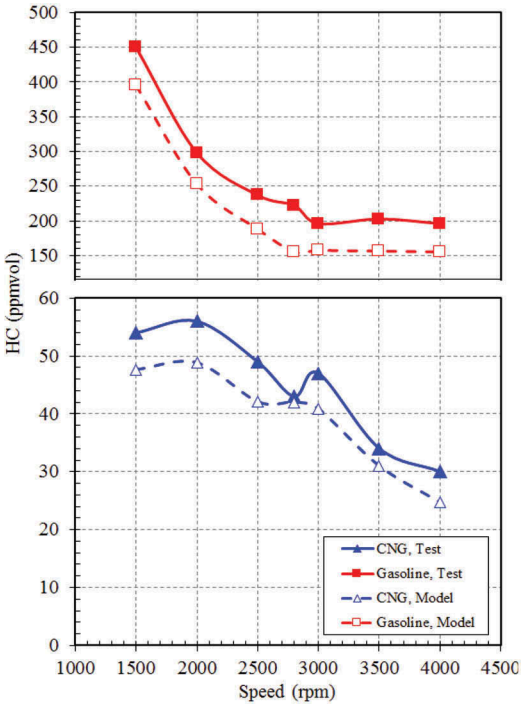

Figure 11. HC emission.

CO emission curves are examined for both fuels, it is seen that the CO emission for CNG is considerably lower (89.7%) than gasoline for both test and model results. The CO_2 emission curves in Figure 9 also support the behavior of CO curves in Figure 10.

As plotted in Figure 11, HC formation, in general, decreases with the engine speed for both fuels. HC formation in spark ignition engines is caused by many reasons; crevices in cylinder, lubrication oil layers, residual bulk gas, cylinder wall temperature, incomplete combustion, chamber shape, valve overlap, secondary air flow (Heywood 1988). Reported HC emission in the literature is 3000 ppmvol for typical naturally aspirated spark ignition engines (Pulkrabek 2004). For Honda L13A4 i-DSI engine, features of two diagonal-positioned spark plugs in each cylinder and sequential ignition ensure that the amount of unburned fuel in the cylinder is at a very low level. Thus, as seen in Figure 11, the HC formation range for this engine is 196–450 ppmvol and 30–54 ppmvol for gasoline and CNG, respectively. These values are considerably smaller than the commonly known value of 3000 ppmvol. For gasoline, as seen in Figure 11, HC formation decreases up to the maximum torque speed of 2800 rpm since the engine designed to give the best fuel performance at this speed. Then, it stays almost constant up to 4000 rpm. The HC formation of 450 ppmvol at 1500 rpm drops to almost half value at 4000 rpm. For CNG, HC formation is very less compared to gasoline. It drops linearly from 54 to 30 ppmvol with increasing engine speed from 1500 rpm to 4000 rpm. The H/C ratio of CNG is higher than gasoline. Gasoline contains more sub-components. Consequently, HC formation for CNG is very less than gasoline. A better air-fuel mixture and combustion are achieved since CNG is fed in gas phase. Another effect is that HC forms during liquid gasoline evaporation. The evaporation delay does not exist for CNG. Consequently, HC formation for CNG is much lower than gasoline.

The NO_x formation versus the engine speed is plotted in Figure 12. The NO_x formation depends on mainly the air–fuel ratio and in-cylinder temperature. As seen in Figure 12, the NO_x formation increases with the engine speed since the in-cylinder temperature rises with the speed as well. The

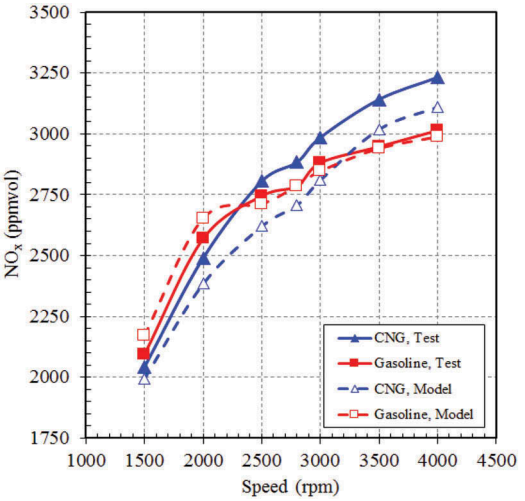

Figure 12. NO_x formation.

NO_x formation range is 2092–3015 ppmvol. and 2042–3233 ppmvol. for gasoline and CNG, respectively. The NO_x formation for CNG at high speeds is higher than gasoline since the CNG has the tendency to work at poor mixtures due to its high H/C ratio. The increasing exhaust gas temperature with the engine speed (Figure 13) supports the increasing the NO_x formation trends for both fuels. The dual sequential ignition of the engine and high compression ratio also elevate the exhaust gas temperature. The NO_x emission for CNG at high speeds is higher than gasoline.

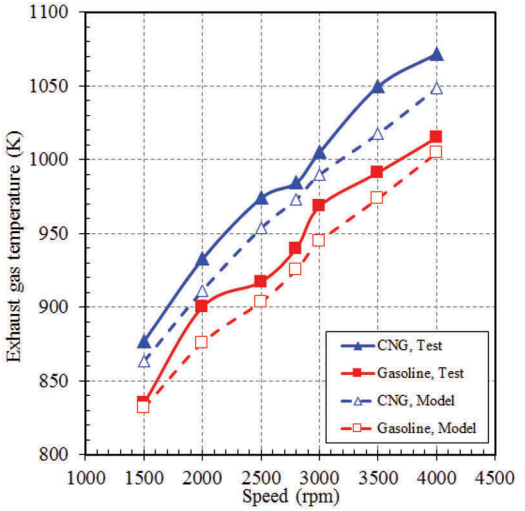

Figure 13. Exhaust gas temperature.

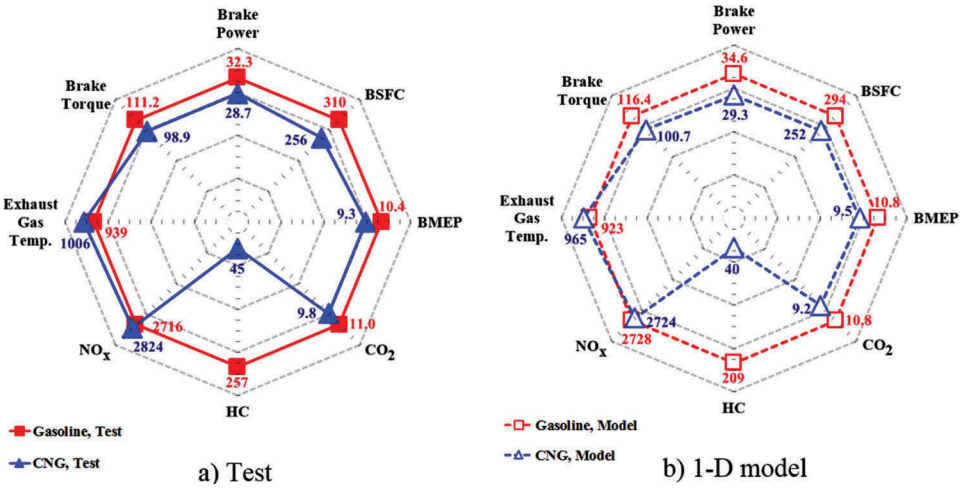

Figure 14. Gasoline and CNG comparison in terms of engine performance and emissions.

Conclusion

In this experimental and numerical study, characteristics of a dual sequential ignition engine were determined for gasoline and CNG fuels at wide open throttle for a speed range of 1500–4000 rpm. Engine performance (brake torque, brake power, brake specific fuel consumption, brake mean effective pressure), emissions (O_2, CO_2, CO, HC, NO_x, and lambda) and the exhaust gas temperature were quantified by testing and modeling the engine. The results from tests and the model have similar tendencies. Overall, the model results were slightly higher than the test results due to the inability to transfer all real test conditions into the idealized model (thermal-flow losses and mechanical losses). The close match with test results validates the model approach. So, the 1-D engine model can be used to estimate the engine behavior for various operating conditions.

Engine characteristics were determined in a speed range of 1500–4000 rpm at wide open throttle. In order to make a projectile comparison between gasoline and CNG, each determined parameter is averaged over the speed range and all parameters are plotted in Figure 14 in a comparative manner. Figure 14 summarizes quantified engine characteristics for the dual sequential ignition engine of Honda L13A4 i-DSI by using test and model results for gasoline and CNG. Overall, CNG usage decreases engine performance except BSFC and emissions except NO_x.

Quantified findings for the specific engine based on test data are summarized, respectively. The brake torque and brake power for CNG are approximately 12% less than gasoline for the considered speed range. As a reason for less torque and power, the BMEP for CNG is 12.8% less. The BSFC is 16.5% lower for CNG. Thus, CNG has advantageous in terms of the amount of fuel that is burned in the engine for 1 kW power generation per hour. The O_2 emission for CNG is approximately 55.4% higher than gasoline. Compared to gasoline, CNG gives approximately 12.1% and 89.7% lower CO_2 and CO emissions, respectively. HC formation for CNG is approximately 475% lower than gasoline. The NO_x emission for CNG at high speeds is higher than gasoline.

Acknowledgment

This work was partially funded by Scientific Research Projects Coordination Unit of Kırıkkale University under project numbers of 2015/100 and 2015/101 through the Automotive Research Laboratory at the Mechanical Engineering Department.

ORCID

Ahmet Alper Yontar http://orcid.org/0000-0002-5453-5137
Yahya Doğu http://orcid.org/0000-0003-0474-2899

References

Alqahtani, A., F. Shokrollahihassanbarough, and M. L. Wyszynski. 2015. Thermodynamic simulation comparison of AVL BOOST and Ricardo WAVE for HCCI and SI engines optimization. *Combustion Engines* 161 (2):68–72.

Aslam, M. U., H. H. Masjuki, M. A. Kalam, H. Abdeselam, T. M. I. Mahlia, and M. A. Amalina. 2006. An experimental investigation of CNG as an alternative fuel for a retrofitted gasoline vehicle. *Fuel* 85:717–24. doi:10.1016/j.fuel.2005.09.004.

Baratta, M., D. Misul, P. Goel, and D. Laurenzano. 2018. Experimental and numerical analysis of diluted combustion in a direct injection CNG engine featuring post-euro-VI fuel consumption targets. *SAE Technical Paper* 01–1142. doi:10.4271/2018-01-1142.

Basha, S. A., and R. K. Gopal. 2009. In-cylinder fluid flow, turbulence and spray models-a review. *Renewable and Sustainable Energy Reviews* 13 (6–7):1620–27. doi:10.1016/j.rser.2008.09.023.

Boretti, A. A., and S. Jiang. 2014. Development of a two stroke direct injection jet ignition compressed natural gas engine. *Journal of Power Technologies* 94:145.

Bozza, F., A. Gimelli, L. Andreassi, V. Rocco, and R. Scarcelli. 2008. 1D-3D analysis of the scavenging and combustion process in a gasoline and natural-gas fuelled two-stroke engine. SAE Technical Paper (No. 2008-01-1087). doi:10.4271/2008-01-1087.

Cheng, W. K., D. Hamrin, J. B. Heywood, S. Hochgreb, K. Min, and M. Norris. 1993. An overview of hydrocarbon emissions mechanisms in spark-ignition engines. *SAE Paper*. doi:10.4271/932708.

Cho, H. M., and H. Bang-Quan. 2007. Spark ignition natural gas engines - a review. *Energy Conversion and Management* 48:608–18. doi:10.1016/j.enconman.2006.05.023.

D'Errico, G., and T. Lucchini. 2005. A combustion model with reduced kinetic schemes for SI engines fuelled with compressed natural gas. SAE Paper No. 2005-01-1123. doi: 10.4271/2005-01-1123.

Delpech, V., J. Obiols, D. Soleri, L. Mispreuve, E. Magere, and S. Kermarrec. 2010. Towards an innovative combination of natural gas and liquid fuel injection in spark ignition engines. *SAE International Journal of Fuels and Lubricants Paper No. 2010-01-1513*. doi:10.4271/2010-01-1513.

Fenimore, C. P. 1970. Formation of nitric oxide in premixed hydrocarbon flames. *Proceedings of the Combustion Institute* 13:373. doi:10.1016/S0082-0784(71)80040-1.

Geok, H. H., T. I. Mohamad, S. Abdullah, Y. Ali, and A. Shamsudeen. 2009. Experimental investigation of performance and emissions of a sequential port injection compressed natural gas converted engine. SAE Paper No. 2009-32-0026.

Ha, J. Y., J. S. Park, and J. H. Kang. 2010. Effects of the throttle opening ratio and the injection timing of CNG on the combustion characteristics of a DI engine. *International Journal of Automotive Technology* 11:11–17. doi:10.1007/s12239-010-0002-8.

Heywood, J. B. 1988. *Internal combustion engine fundamentals*. New York: McGraw-hill college.

Hooper, P. R., T. Al-Shemmeri, and M. J. Goodwin. 2012. An experimental and analytical investigation of a multi-fuel stepped piston engine. *Applied Thermal Engineering* 48:32–40. doi:10.1016/j.applthermaleng.2012.04.034.

Jahirul, M. I., H. H. Masjuki, R. Saidur, M. A. Kalam, M. H. Jayed, and M. A. Wazed. 2010. Comparative engine performance and emission analysis of CNG and gasoline in a retrofitted car engine. *Applied Thermal Engineering* 30:2219–26. doi:10.1016/j.applthermaleng.2010.05.037.

Lim, G., S. Lee, C. Park, Y. Choi, and C. Kim. 2013. Effects of compression ratio on performance and emission characteristics of heavy-duty SI engine fuelled with HCNG. *International Journal of Hydrogen Energy* 38:4831–38. doi:10.1016/j.ijhydene.2013.01.188.

Mahle GmbH. 2012. *Pistons and engine testing*. Stuttgart: ATZ/MTZ-Fachbuch.

Mahrous, A. M., A. Potrzebowski, M. L. Wyszynski, H. M. Xu, A. Tsolakis, and P. Luszcz. 2009. A modelling study into the effects of variable valve timing on the gas exchange process and performance of a 4-valve DI homogeneous charge compression ignition (HCCI) engine. *Energy Conversion and Management* 50:393–98. doi:10.1016/j.enconman.2008.09.018.

Migita, H., T. Amemiya, K. Yokoo, and Y. Iizuka. 2002. The new 1.3-liter 2-plug engine for the 2002 Honda fit. *JSAE Review* 23:507–11. doi:10.1016/S0389-4304(02)00235-7.

Movahed, M. M., T. H. Basirat, and M. Mirsalim. 2014. Experimental investigation of the concomitant injection of gasoline and CNG in a turbocharged spark ignition engine. *Energy Conversion and Management* 80:126–36. doi:10.1016/j.enconman.2014.01.017.

Nakayama, Y., M. Suzuki, Y. Iwata, and J. Yamano. 2001. Development of a 1.3 lt 2-plug engine for the 2002 model fit. *Honda R&D Technical Review* 13:43–52.

Newhall, H. K. 1968. Kinetics of engine-generated nitrogen oxides and carbon monoxide. *Proceedings of 12th International Symposium on Combustion 603-613*. doi:10.1016/S0082-0784(69)80441-8.

Obiols, J., D. Soleri, N. Dioc, and M. Moreau. 2011. Potential of concomitant injection of CNG and gasoline on a 1.6 lt gasoline direct injection turbocharged engine. SAE Paper No. 2011-01-1995. doi:10.4271/2011-01-1995.

Pipitone, E., and S. Beccari. 2009. Performances improvement of a SI CNG bi-fuel engine by means of double-fuel injection. SAE Paper No. 2009-24-0058. doi:10.4271/2009-24-0058.

Pulkrabek, W. W. 2004. *Engineering fundamentals of the internal combustion engine*. New Jersey: Pearson prentice hall.

Putrasari, Y., A. Praptijanto, A. Nur, B. Wahono, and W. B. Santoso. 2015. Evaluation of performance and emission of SI engine fuelled with CNG at low and high load condition. *Energy Procedia* 68:147–56. doi:10.1016/j.egypro.2015.03.243.

Ricardo Wave 2015. 2015. *2, Manual, Ricardo-Suite*.

Sjöberg, M., and J. E. Dec. 2004. An investigation of the relationship between measured intake temperature, BDC temperature, and combustion phasing for premixed and DI HCCI engines. SAE Technical Paper (No. 2004-01-1900). doi:10.4271/2004-01-1900.

Thipse, S. S., S. D. Rairikar, K. P. Kavathekar, and P. P. Chitnis. 2009. Development of a six cylinder HCNG engine using an optimized lean burn concept. SAE Paper No. 2009-26-0031. doi: 10.4271/2009-26-0031.

Varde, K. S., and G. M. Asar. 2001. Burn rates in natural gas fueled single cylinder spark ignition engine. SAE Paper No. 2001-28-0023. doi:10.4271/2001-28-0023.

Verma, G., R. K. Prasad, R. A. Agarwal, S. Jain, and A. K. Agarwal. 2016. Experimental investigations of combustion, performance and emission characteristics of a hydrogen enriched natural gas fuelled prototype spark ignition engine. *Fuel* 178:209–17. doi:10.1016/j.fuel.2016.03.022.

Vibe, I. I. 1956. Semi-empirical expression for combustion rate in engines. In Proceedings of Conference on piston engines. USSR academy of sciences Moscow, 185–91.

Wang, X., H. Zhang, B. Yao, Y. Lei, X. Sun, D. Wang, and Y. Ge. 2012. Experimental study on factors affecting lean combustion limit of SI engine fueled with compressed natural gas and hydrogen blends. *Energy* 38:58–65. doi:10.1016/j.energy.2011.12.042.

Woschni, G. 1967. Universally applicable equation for the instantaneous heat transfer coefficient in the internal combustion engine. SAE Paper. doi:10.4271/670931.

Xu, S., D. Anderson, A. Singh, M. Hoffman, R. Prucka, and Z. Filipi. 2014. Development of a phenomenological dual-fuel natural gas diesel engine simulation and its use for analysis of transient operations. *SAE International Journal of Engines* 7(2014–01–2546):1665–73. doi:10.4271/2014-01-2546.

Yadollahi, B., and M. Boroomand. 2013. The effect of combustion chamber geometry on injection and mixture preparation in a CNG direct injection SI engine. *Fuel* 107:52–62. doi:10.1016/j.fuel.2013.01.004.

Yontar, A. A., and Y. Doğu. 2016. 1-D modelling comparative study to evaluate performance and emissions of a spark ignition engine fuelled with gasoline and LNG. *MATEC EDP Sciences* 81:05003. doi:10.1051/matecconf/20168105003.

Zheng, J. J., J. H. Wang, B. Wang, and Z. H. Huang. 2009. Effect of the compression ratio on the performance and combustion of a natural-gas direct-injection engine. *Proceedings of the institution of mechanical engineers, part d: Journal of automobile engineering* 223:85–98. doi: 10.1243/09544070JAUTO976.